EURECA – A European-Japanese micro-calorimeter array

Piet A.J. de Korte[*a], Jose V. Anquita[b], Xavier Barcons[c], Paolo Bastia[d], Joern Beyer[e], Fernando Briones[b], Marcel Bruijn[a], Javier Bussons[f], Augustin Camón[i], F. Carrera[c], Maria Teresa Ceballos[c], Luca Colasanti[o], Bob Dirks[a], Dietmar Drung[e], Lourdes Fabrega[h], Flavio Gatti[j], Raquel Gonzalez-Arrabal[b], Luciano Gottardi[a], Wojtek Hajdas[k], Panu Helistö[l], Jan-Willem den Herder[a], Henk Hoevers[a], Yoshitaka Ishisaki[m], Mikko Kiviranta[l], Jan van der Kuur[a], Claudio Macculi[o], Aliko Mchedlishvili[k], Kazu Mitsuda[n], Stéphane Paltani[g], Maria Parra-Borderías[i], Luigi Piro[o], Reiner Rohlfs[g], Javier Sese[p], Yoh Takei[n], Guido Torrioli[q], Noriko Yamasaki[n],

[a]SRON Netherlands Institute for Space Research, Sorbonnelaan 2, 3584CA Utrecht, Netherlands; [b]IMM-Instituto de Microelectronica de Madrid,C/Isaac Newton, 8(PTM)28760-Tres Cantos, Madrid [c]Instituto de Fisica de Cantabria, Edificio Juan Jorda, Avenida de los Castros s/n, E-39005 Santander, Cantabria, Spain; [d]Thales Alenia Space S.p.A., S.S. Padana Superiore 290, I 20090 Vimodrone (Milano), Italy; [e]Physikalisch-Technische Bundesanstalt, Abbestrasse 2-12, D-10587 Berlin, Germany; [f]University of Murcia, Murcia, Spain; [g]ISDC, 16 ch. d'Ecogia, CH-1290 Versoix, Switzerland; [h]Institut de Ciència de Materials de Barcelona (CSIC), Campus de la UAB, 08193 Bellaterra, Spain; [i] ICMA- Instituto de Ciencia de Materiales de Aragón, CSIC- Universidad de Zaragoza, Pedro Cerbuna 12, 50009 Zaragoza, Spain; [j]INFN and University of Genoa, Via Dodecaneso 33, 16146 Genoa, Italy; [k]Paul Scherrer Institut, 5232 Villigen PSI, Schweiz; [l]VTT Sensors, P.O. Box 1000, FIN-02044 VTT, Finland; [m]Tokyo Metropolitan University, 1-1 Minami-Osawa, Hachioji, Tokyo, 192-0397, Japan; [n]Institute of Space and Astronautical Science (ISAS/JAXA), 3-1-1 Yoshinodai, Sagamihara, Kanagawa 229-8510, Japan;[o]Istituto Astrofisica Spaziale Fisica Cosmica, INAF, Via Fosso del Cavaliere I-00133 Roma, Italy; [p]INA - Instituto Universitario de Investigación en Nanociencia de Aragón, Universidad de Zaragoza, C/ Pedro Cerbuna 12, 50009 Zaragoza, Spain; [q]Institute for Photonics and Nanotechnologies (CNR), Via Cineto Romano 42, 00156 Roma, Italy

ABSTRACT

The EURECA (EURopean-JapanEse Calorimeter Array) project aims to demonstrate the science performance and technological readiness of an imaging X-ray spectrometer based on a micro-calorimeter array for application in future X-ray astronomy missions, like Constellation-X and XEUS. The prototype instrument consists of a 5 x 5 pixel array of TES-based micro-calorimeters read out by by two SQUID-amplifier channels using frequency-domain-multiplexing (FDM). The SQUID-amplifiers are linearized by digital base-band feedback. The detector array is cooled in a cryogen-free cryostat consisting of a pulse tube cooler and a two stage ADR. A European-Japanese consortium designs, fabricates, and tests this prototype instrument. This paper describes the instrument concept, and shows the design and status of the various sub-units, like the TES detector array, LC-filters, SQUID-amplifiers, AC-bias sources, digital electronics, etc.

Initial tests of the system at the PTB beam line of the BESSY synchrotron showed stable performance and an X-ray energy resolution of 1.58 eV at 250 eV and 2.5 eV @ 5.9 keV for the read-out of one TES-pixel only. Next step is deployment of FDM to read-out the full array. Full performance demonstration is expected mid 2009.

Keywords: X-ray astronomy, X-ray instrumentation, cryogenic radiation detectors, X-ray micro-calorimeters, SQUIDs, frequency-domain-multiplexing.

[*]P.A.J.de.Korte@sron.nl; phone +31 30 2535710; fax +31 30 2540860, www.sron.nl

Space Telescopes and Instrumentation 2008: Ultraviolet to Gamma Ray, edited by Martin J. L. Turner, Kathryn A. Flanagan, Proc. of SPIE Vol. 7011, 701122, (2008) · 0277-786X/08/$18 · doi: 10.1117/12.788963

1. INTRODUCTION

EURECA (**EUR**opan-Japan**E**se **C**alorimeter **A**rray) is a multi-national European-Japanese project that aims to demonstrate technical readiness of a Transition-Edge-Sensor (TES) based X-ray imaging spectrometer for application on future X-ray astronomy missions, like ESA's XEUS, JAXA's DIOS, and NASA's Constellation-X. Besides the development of large detector arrays this requires the development of multiplexed read-out electronics to reduce the heat load onto the cryostat by a smaller number of wires in the interconnecting harness, and active electronics components, like SQUID-amplifiers, at cryogenic temperature. The extreme sensor sensitivity demands great care with EMC (electro-magnetic compatibility), thereby enforcing careful design of grounding, shielding, and filtering. Of crucial importance are also the cooler and instrument chamber design.

Fig. 1 gives an impression of the various components within the EURECA project. Cooling to about 50 mK is realized by means of a commercial pulse-tube cooler in combination with a two-stage adiabatic demagnetization refrigerator (ADR). The sensor is a 5 x 5 pixel TES micro-calorimeter array with 250 x 250 μm^2 pixels, aiming at an energy resolution of < 2 eV for the < 2 keV energy range and 5 eV @ 7 keV in combination with 100 µs response time. The array will be read-out by two SQUID-based amplifier chains on the basis of frequency-domain-multiplexing (FDM). This requires an LC-filter for each pixel and two SQUID amplifiers. These are mounted together with the detector array into a so-called cold head, which is cooled by connection to the cold finger of the ADR. The SQUIDs will be read-out by low-noise-amplifiers (LNAs) and operated in a digital base-band feedback circuitry, to linearize the SQUID response and increase its dynamic range. FDM requires AC-bias of the detectors, and therefore de-modulation of the summed output signal to retrieve of the signals from the individual pixels. Signal processing will be required to extract the X-ray energy from the data stream.

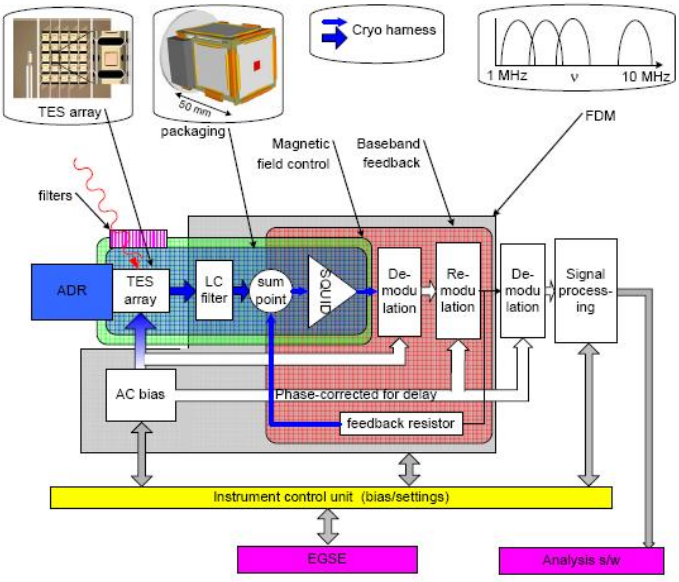

Fig. 1: EURECA Schematic

2. TES ARRAY

EURECA will use a 5 x 5 TES-array[1]. Such detector arrays based on bulk-micromachining[2] have been successfully produced (Fig. 2) and individual pixels show an energy resolution about 2.5 eV FWHM for 5.9 keV X-rays. The pixels in these arrays have a 250 x 250 μm^2 size and each pixel a 160 x 160 μm^2 Ti/Au TES with a transition temperature at about 100 mK. The mushroom shaped Cu/Bi absorber will be coupled to the 100 x 100 μm^2 central area of the TES by means of a copper stem. The absorber-TES configuration sits on top of a 1 µm Si_3N_4-membrane, which leads to about 6 pW bias power for a 50 mK bath temperature. For future applications (XEUS), the first 32 x 32 array has been successfully manufactured, but could not been tested since a production failure damaged the electrical interconnections.

The detector array requires a large absorption efficiency and high filling factor for the energy range 0.1 – 10 keV. A photo-resist process has been developed for the production of mushroom shaped absorbers consisting of a 150 nm Cu base and a 2.8 µm Bi top layer (Fig. 3). So far the performance has been tested for stacked (i.e. not with a mushroom shape) Cu/Bi absorbers (with respective thicknesses of 1 µm and 2.8 µm) and a 100 x 100 μm^2 footprint on the TES. The energy resolution obtained with these devices cases equals 2.5 eV @ 5.9 keV.

Recently crosstalk measurements have been performed on the 5 x 5 arrays. When irradiating one pixel with a thermo-electrical pulse the response of the neighboring pixels has been measured to be a about of 5 10^{-4} and 7 10^{-6} for the nearest neighboring pixel on the other side of the support beams (horizontal in Fig.2) and the nearest neighboring pixel along the diagonal, respectively.

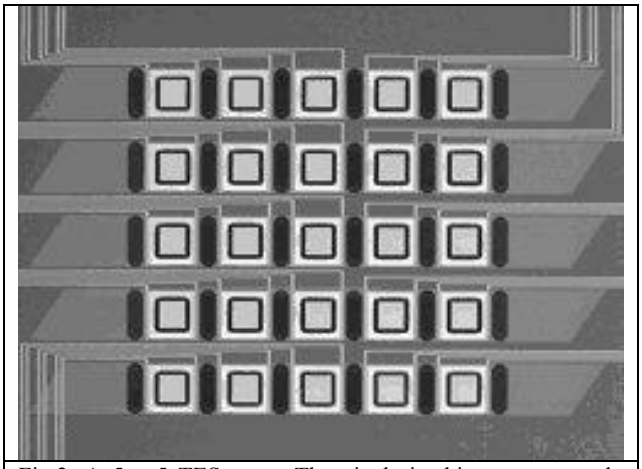

Fig.2. A 5 x 5 TES-array. The pixels in this array are only equipped with the central Cu-stem of the absorber. The Cu/Bi hood has still to be manufactured.

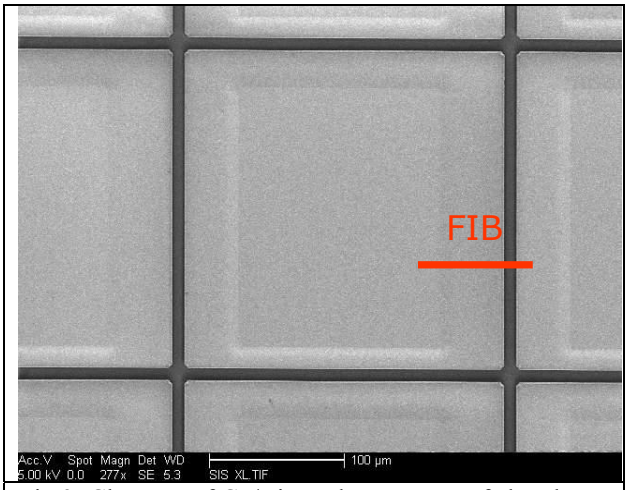

Fig.3: Close-up of Cu/Bi Mushroom type of absorbers on a 5 x 5 pixel array

3. FREQUENCY-DOMAIN-MULTIPLEXED READ-OUT

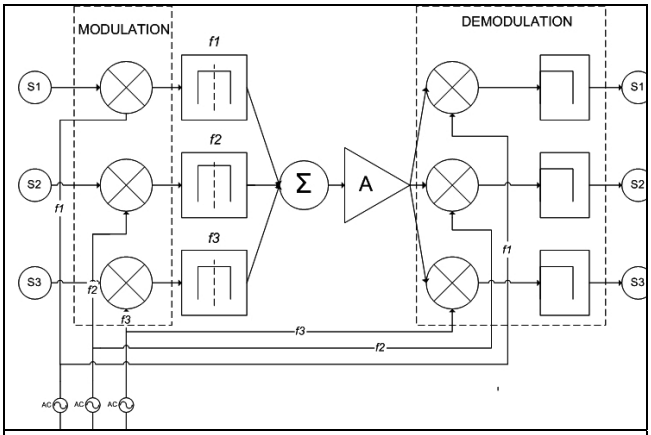

Fig. 4 Principle of FDM. The respective signals s_1, s_2, s_3 are modulated by sin-functions at frequencies f_1, f_2, f_3. Subsequently the amplitude modulated carriers are summed and amplified. Before summing band filters at each pixel are required to prevent addition of wideband noise. Demodulation of the summed and amplified signal is achieved by multiplication with the respective carriers at frequencies f_1, f_2, f_3 again and subsequent low pass filtering to remove the other pixels and higher harmonics.

Multiplex techniques make use of the fact that for most applications the bandwidth of an amplifier chain is larger than the information bandwidth of one information unit, in our case that of one TES-pixel. So the large bandwidth of amplifier and harness can be used to amplify and transport the information of several pixels by fingerprinting the information of each pixel such that the information is not impaired. In multiplexing schemes signals are multiplied by an orthogonal set of modulating functions $f_1(t)$, $f_2(t)$, ..., acting as unique fingerprints, and are subsequently summed and read-out by a single amplifier chain. The individual signals can be recovered when the summed signal is multiplied by the modulating functions again and low pass filtered.

In practice both time-domain-multiplexing (TDM) and frequency-domain-multiplexing (FDM) are under development for the read-out of TES-arrays. An overview[4] of both technologies has been given at LTD-11. TDM is pioneered by the cryogenic detector group at NIST, Boulder[5,6,7]. FDM is under development at Berkeley[8], ISAS[9], and SRON[10,11] .

3.1 Principle of Frequency-Domain-Multiplexing

The principle of frequency-domain-multiplexing (FDM) is shown in Fig.4. When used for the read-out of TES arrays it is logical to use the TES itself as amplitude modulator by biasing it with an AC-bias signal instead of the generally used

DC-bias. In that case noise band filters are naturally formed by the LC circuit required to voltage bias the TES at $f = 1/2\pi\sqrt{LC}$. Both SRON[12], LLNL[13], and Berkeley[8] have shown that AC-bias operation of TES sensors allows for X-ray energy resolutions close to those obtained by means of DC-bias of the same devices. Also multiplexing has been shown without significant loss of performance.

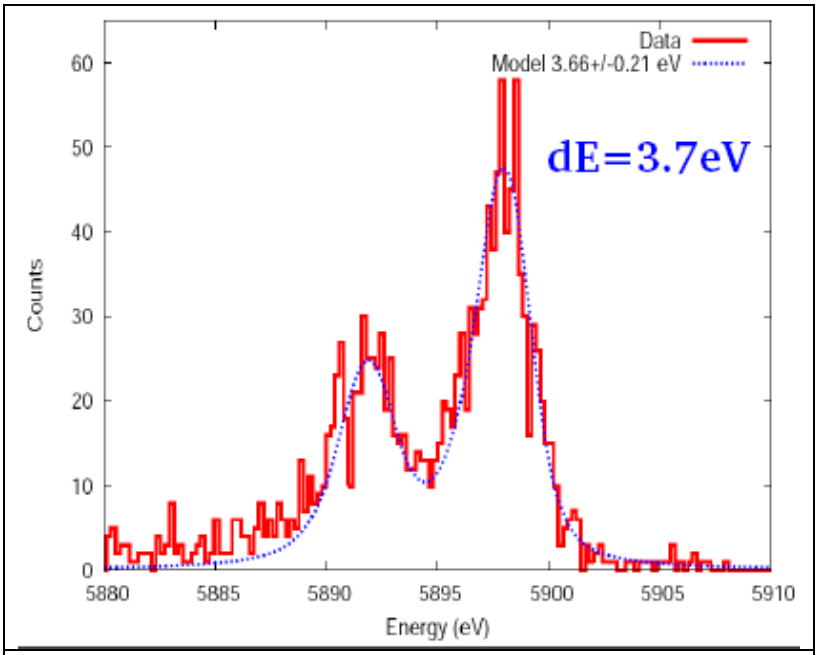

Fig.5: Energy spectrum of Mn-Kα1,2 observed under about 400 kHz AC-bias. The drift corrected energy resolution equals 3.7 eV for a baseline resolution equal to 3.5 eV.

Recently SRON has measured energy resolution for AC-biased pixels in a 5 x 5 array, giving an energy resolution of 2.5 eV @ 5.9 keV when DC biased. The experiment has been performed at 400 kHz bias-frequency. This data suffered from short term and long term drifts up to about 10 eV, most probably originating from the AC-bias generator (short term) and the ADR remnant magnetic field (long term). Using the strong correlation between the pre-pulse and peak signal level a drift correction has been applied to the data shown in Fig.5. The obtained energy resolution under AC-bias equals 3.7 eV @ 5.9 keV, while the baseline resolution equals 3.5 eV. The origin of the extra noise compared to that measured DC-operation is not yet fully understood.

3.2 Summing Topology

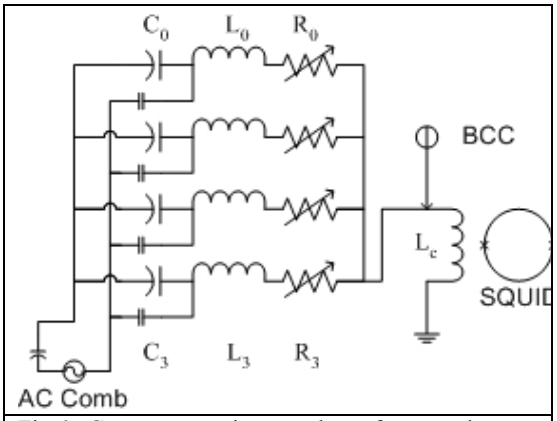

Fig.6: Current summing topology for one detector column, showing also the capacitive coupling of the bias comb and the common impedance of the summing point

Summing of the signals can be done in several ways. The group at Berkeley[14] started out with voltage summing using a summing loop. At present all groups working with FDM make either use of flux summing[15] or current summing[10]. The current summing approach is shown in Fig. 6., which is baseline for EURECA. The bias current is supplied as a bias comb per column, making use of only one twisted wire-pair. In this design the LC-filters separate the bias frequencies in the comb to the individual pixels. Since the LC-filters are not extremely steep this results in multi-tone biasing of each pixel. For a typical frequency spacing of 200 kHz this results in power crosstalk < 10^{-4}, but current signals at neighboring frequencies at about 10^{-2} of the main frequency. This can be significantly improved by using two or more bias leads, so that the frequency separation can be enlarged. The bias voltage is supplied by use of capacitive coupling, thereby generating a voltage source over the capacitance of the LC-filter. Biasing per column allows for frequency adjustment per pixel at the expense of a bias source per pixel.

3.3 Bias Current Cancellation

Since in FDM all pixels are on continuously the AC-bias signals add, eating a very significant part of the dynamic range of the amplifier chain. To alleviate this one can make use of offset removal, generally called bias current cancellation (BCC) by applying a compensation current at the SQUID input, so that current is fed to the SQUID-amplifier input only in case a signal is present at one or more pixels.

In case of EURECA the digital base-band feedback loop is expected to take care of the required bias-current suppression, since for that system the feedback loop gain is very high at each bias frequency.

3.4 FDM Performance Characteristics

The FDM performance[11] is largely determined by the dynamic range and bandwidth of the X-ray events in each TES sensor, the dynamic range and bandwidth of the SQUID amplifier chain, and limiting factors like crosstalk due to SQUID nonlinearity, channel frequency separation, etc. The crosstalk levels for the FDM electronics do not have to be significantly better than that in the detector array itself.

3.4.1 Dynamic Range

The dynamic range of the TES-sensor under AC-bias is given by $\Delta I / i_n \approx \pm\sqrt{P / nkT}$ with ΔI the maximum current change due to absorption of an X-ray photon, and i_n the noise level of the TES. P is the bias power dissipated in the TES, and $n \approx 3 - 4$ the exponent of the thermal conductance to the bath. For XEUS the TES dynamic range is typically +/- 10^6 $Hz^{1/2}$. Given the use of BCC, the relative small number of coincident events in one column, and the generally steep X-ray energy spectra for astronomical sources, the required dynamic range for one column is at most about twice that of a single pixel. Obviously the electronics has to be significantly better, resulting in an electronics dynamic range requirement of about 5 10^6 $Hz^{1/2}$. The dynamic range achievable with a SQUID amplifier, i.e.: +/- 0.1 Φ_0/Φ_n, is set by the flux noise Φ_n of the SQUID amplifier. Till recently SQUID flux noise levels of about 1 $\mu\Phi_0/Hz^{1/2}$ were quite common. More recent developments show that noise levels as low as 0.1 and 0.16 $\mu\Phi_0/Hz^{1/2}$ are achievable for single SQUIDs[17], and array SQUIDs[18,19], respectively. This creates a SQUID dynamic range of approximately +/- 10^6 $Hz^{1/2}$. This value is slightly worse than the dynamic range of the input signal. One of the most obvious ways to solve this is by using feedback to the SQUID input with a modest loop gain of $(5 – 10)$[20].

3.4.2 Signal bandwidth, channel separation, cross talk, and frequency range

The bandwidth requirement for FDM depends on the number of pixels in one read-out channel and the frequency separation between channels. The maximum signal bandwidth (risetime) for slightly overdamped pulses with an effective fall time of 100 μs (1.6 kHz) equals approximately 5 and 16 kHz for small and large signals, respectively. In our design the filter coil L = 1 μH and the TES bias point resistance of 40 mΩ .

The channel separation is limited by several factors. One of those is the crosstalk between neighbouring frequency bins, which gets caused by: (1) multi-tone biasing of the pixels, since the LCR filters are not steep enough to fully separate the biascomb; (2) common impedance L_c of the summing node (Fig.5); (3) signal information is not truly bandwidth limited.

For a typical 200 kHz separation crosstalk levels up to 0.2%, e.g. 12 eV for a 6 keV X-rays, are present. So in case of coincident events in neighboring frequency pixels corrections will be required. Given the maximum count rate per pixel for good spectroscopy (typically few 100 c/s for XEUS) only typically about one percent of the events will be coincident, so one could discard those events.

The frequency range usefull for FDM equals about 1 – 10 MHz. Below 1 MHz frequency the capacitance of the LC-filters get quite bulky, while the gain in extra number of channels is very limited. The upper frequency of 10 MHz is crudely set by: (1) SQUID backaction noise corner frequency; (2) LC – filter quality, i.e. the equivalent series resistance (R_{ESR}) of the LC-filters has to be smaller than the TES bias resistance, so that Q > 628 f (MHz), (3) phase rotation in wiring harness and amplifiers.

Cross talk due to SQUID nonlinearity is only important for coincident events. The fraction of these type of events is small and can be neglected. The use of feedback for linearisation actually reduces these effects quadratically and to the third power with the feedback loop gain for 2nd and 3rd order harmonics, respectively.

3.5 Base-band feedback for dynamic range enhancement and linearization of the SQUID response

Several ways exist to linearize SQUIDs. For standard applications the use of a Flux-Locked-Loop (FLL) is used. Due to signal delay and phase rotation in the cabling between warm electronics and the SQUID cold-amplifiers the maximum gain bandwidth for those systems is typically 20 MHz, allowing for very moderate loop gain in the 1 – 10 MHz range. Other approaches presented in the past are feed-forward and base-band feedback. For EURECA the use of base-band feedback has been chosen.

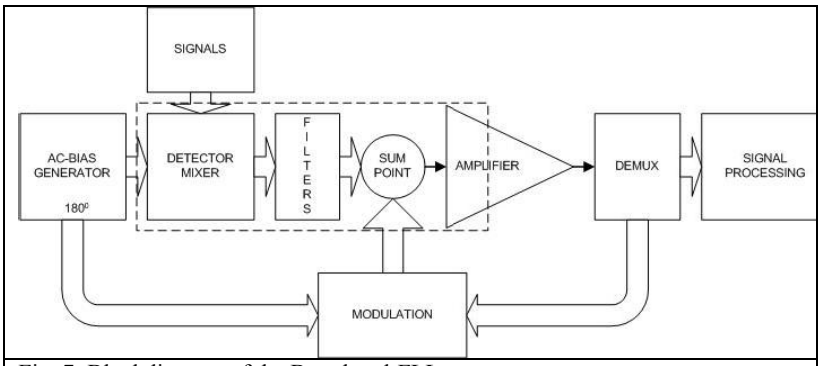

Fig. 7: Blockdiagram of the Base band-FLL system

An overall block diagram of the "base band feedback" concept for the read-out of an X-ray spectrometer is shown fig. 7. For each read-out column demodulation of all M signals after amplification is required. After single pole filtering using an integrator the signals are modulated again with the carriers and subsequently fed back to the summing point. The phase of the carriers used for re-modulation are compensated for cable delays and phase rotations such that a stable feedback loop with appreciable loop gain is created in a frequency band around the central carrier frequency. In this way the full 1- 10 MHz frequency range becomes available for FDM.

On basis of the realizable delay in such a digital feedback system, typically 250 ns, the estimated gain-bandwidth for a single frequency loop equals $0.08/t_{delay}$ = 320 kHz, which would allow for a feedback loop gain of 32 @ 10 kHz. The close packing of the various carriers does however result in summing of amplitude and phase of the contibutions from all frequency channels, thereby reducing the maximum loop gain while maintaining a 60 degree phase margin.

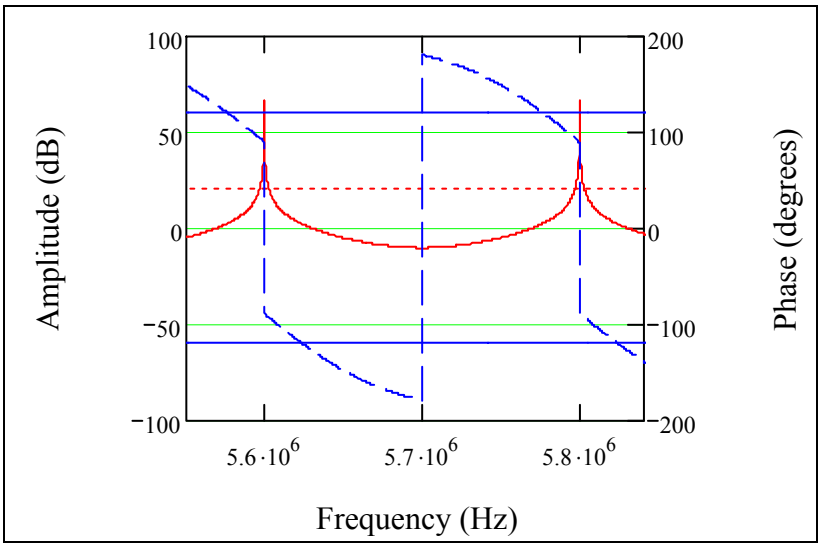

Fig. 8: Maximum feedback loop gain achievable for a BBFB system with 44 pixels at a 200 kHz spacing with 60 degrees phase margin. Both amplitude gain and phase are shown for the two central frequencies in the system

A simulation for 44 pixels at a frequency seperation of 200 kHz (Fig. 8) shows that the feedback loop gain possible for 60 degree phase margin equals about 3x at 10 kHz and 20x at 1.6 kHz. The loop gain of the feedback circuit is in first approximation inversely proportional to the frequency spacing of the pixels. So multiplexing of less pixels in the 1 – 10 MHz band results in a larger dynamic range to handle the signals.

Simulations for SQUIDs with a 0.2 $\mu\Phi_0/\sqrt{Hz}$ noise floor and consequently a maximum signal of 1 Φ_0 show that the maximum error signal at the SQUID input will equal about 0.4 Φ_0 for the signal risetime and about 0.02 Φ_0 for the signal falltime. The content of the higher harmonics in that case contain about $8\ 10^{-3}$ and $8\ 10^{-4}$ for the 2nd and 3rd order in case the 2nd and 3rd order polynomial coefficients, describing the SQUID V/I – Ø around its bias point, are equal to that of the 1st order. Most critical in the present system is the strong requirement on the SQUID dynamic range, which can be relaxed by increasing the base-band feedback loop gain at the expense of the number of pixels that can be multiplexed in one channel.

Another approach for linearization and dynamic range increase based on local feedback, by means of cryogenic amplification, the so-called double-loop (DL-FLL) technique is under development at INAF/CNR/TAS.

4. EURECA DESIGN

4.1 System Level

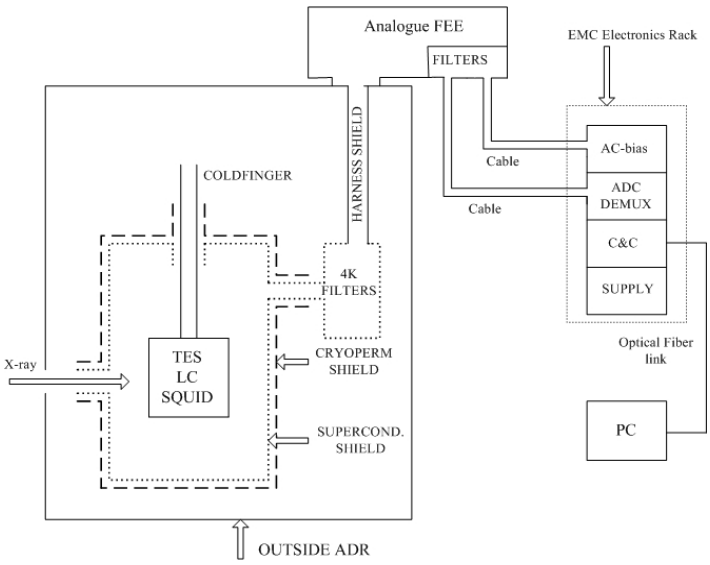

Fig. 9: System design of the EURECA instrument

One of the key issues for the design of the EURECA instrument is its EMC in a "dirty" laboratory environment. Absorption of EM disturbances in the TES at the level of a few fW is equivalent an unacceptable degradation of the energy resolution at the level of eV's. On the basis of experience with TES-based laboratory experiments we have designed EURECA as sketched in Fig. 9. The EURECA electronics housing together with the shielding of the cold head, containing the TES array, the LC-filters, and the SQUIDs, forms a Faraday cage. The cold head shielding consists of an outer cryoperm shield and an inner lead-tin plated copper superconducting shield. The entry port for X-ray radiation will be shielded by a metal grid and the incoming ADR-coldfinger will be electrically shorted to the superconducting shield. The harness from the front end electronics (FEE) is filtered at 4K in a superconducting box that is intimately connected with the superconducting shield of the cold head. Furthermore the harness between 4K and room temperature is fed through a gold-coated stainless steel tube. To reduce common mode disturbances the harness is made out of twisted-wire pairs that are operated differentially.

This system has been extensively tested in the laboratory and at the BESSY synchrotron and in general the system response is not sensitive to extern disturbances. The presence of slow gain drifts (< 10 eV) during long data accumulation periods (hours) might still be due to insufficient shielding of the ADR magnetic field, although thermally induced drifts in the SQUID response cannot be excluded yet.

The electronics inside the FEE-box is low-frequency analogue electronics, either running on batteries fed from the supplies in the electronics rack or directly from that supply. Inside the FEE-box the electronics will be single point grounded to the case.

In the EMC electronics rack each SQUID-channel has two cards: (1) the AC-bias card, containing 8 bias sources for AC-bias and also 8 bias sources for BCC, which are not needed in case base-band feedback is implemented; (2) the ADC/DEMUX card contains two ADC's for data digitization and an FPGA for numerical de-multiplication of the digital data, as well re-modulation with phase compensated carriers for base-band feeedback. The board also contains two DAC's of which one can be used to generate the analogue feeedback signal calculated by the FPGA.

Both cards are connected to the FEE-electronics by well shielded cables and the incoming lines from the rack are filtered upon entering the FEE-box. Since EURECA will have two channels the ADR contains two FEE-boxes and the rack two AC-bias and four DEMUX cards. Control of the instrument and transport of data is in 1st instance by a PC coupled to the rack through an optical fiber connection.

4.2 Adiabatic Demagnetization Refrigerator and Instrument Shielding

For cooling the instrument use is made of a commercial ADR pre-cooled by a CryoMech pulse-tube cooler. Inside this cooler the shielding of the instrument is realized as conceptually shown in Fig. 9. The electrical connections for the operation of the ADR itself, magnet currents and thermometry, are kept outside this instrument enclosure and are well filtered when entering the ADR. Another significant source of electrical disturbance is the valve-head of the pulse-tube cooler and its electrical supply[22]. In the standard dry ADR of Janis the valve-head is hard mounted on top of the pulse-tube and the valve-head supply is mounted inside the CryoMech compressor unit. For EURECA CryoMech has disconnected and galvanically isolated the valve-head from the pulse-tube by one meter of plastic tubing at the expense of 10% cooling power. Furthermore the valve-head power supply has been taken out of the CryoMech compressor unit and integrated with the valve-head unit. This modified valve-head/supply unit is shielded in order to suppress electro-magnetic radiation. The data indicate that this operation has been successful. The margin with respect to vibration induced instrument degradation is however quite small.

4.3 Cold Head

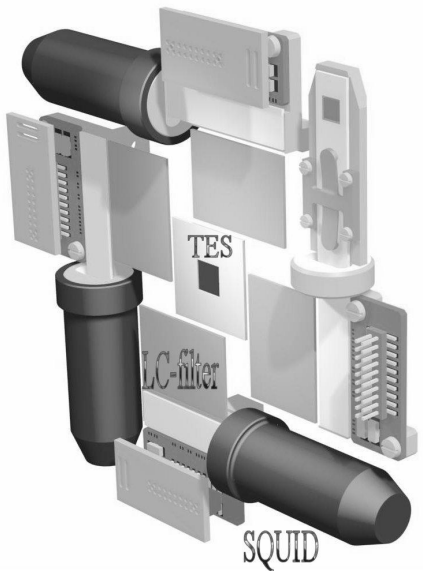

Fig. 9: Cold Head design

The original cold head design is shown in Fig. 10. In the center sits the 5 x 5 detector array on its carrier, equipped with 2 x 8 bondpads at four sides. This central chip is surrounded by four LC-filter chips, each containing 8 LC-filters, and 8 capacitors for coupling the AC-bias (Fig. 5). On the outside are four SQUIDs in superconducting shields of Pb-Sn coated Cu. The interconnection between SQUIDs and LC-filters is made by a Si-interconnection board running in and out the Pb-Sn coated shield, and layed out such that the common inductance in the circuit is minimized. Finally four connectors are the interface for the twisted-wire pair harness for each of the instrument quarters. EURECA will only implement two of the four channels shown.

4.3.1 Detector Array

The TES array ismounted onto a Cu substrate for optimum connection to the coldbath. The pixel connections with be fanned to the outer rim of the wafer to enable wire bonding to the LC-filter chips.

4.3.2 LC Filters

Since TES operation requires voltage bias the LC-filters should have a low series resistance, i.e. < few mΩ. This requirement means that the LC-circuit should have a quality factor $Q > 628\,f$ (MHz). Therefore inductors, capacitors, and electrical leads in the bias circuit are made of superconducting Nb. We found that the high dielectric constant oxides of Nb and Ta are quite lossy, so we presently fabricate LC-filters by using 10 - 20 nm thick Al_2O_3 with $\varepsilon_R \approx 6$ for the capacitors. A lower limit for the Q of the LC-filters of 4000 has been measured at 4 K. For those filters the limited current density of the coils (step coverage problems) prohibited measurements with sufficient signal power resulting in a lower limit for the filter Q only. Meanwhile the step coverage problem has been solved and critical currents are at least several mA, while typical bias currents are 10 μA.

Notwithstanding those improvements the filter production is still not stable and reproducable. A tri-layer process in which the base-electrode, the isolating dielectric, and the top electrode of the capacitor can be deposited in situ without breaking the vacuum is presently implemented.

Accomodation of the LC-filters in the cold head is influenced by their size. In case of a 32 x 32 imaging spectrometer for XEUS and FDM operation in the 1 – 10 MHz range the required net filter surface area equals approximately 37 cm^2. For EURECA the accomodation is shown in Fig. 10.

4.3.3 SQUIDs

SQUIDs should be optimized for the highest possible dynamic range and have an as low as possible input inductance for the required < 6 pA/Hz$^{1/2}$ input current noise, i.e.: a low coupled energy. PTB[18,19] has developed SQUIDs close to the EURECA requirements, i.e. a 16-SQUID array with a flux noise of about 0.16 μΦ/Hz$^{1/2}$ @ 0.3 K. The single turn input coil has an impedance of about 3 nH including stray inductance, resulting in a current noise of 4.5 pA/Hz$^{1/2}$. The output noise temperature of this device is about 30K for an output impedance of 100 Ω. Direct read-out of this SQUID by a low-noise RT amplifier is just possible without significant degradation of the input noise level of the SQUID.

Recently VTT and PTB got funded through an ESA TRP contract to develop SQUID amplifiers with enhanced performance. Optimizations ask for a better coupled energy resolution, larger dynamic range, and higher output noise temperature. A two-stage SQUID system seems the best way to go.

4.4 Electronics

4.4.1 Front End Electronics Box

The signal-electronics in the FEE-box is standard FLL-electronics[20]. For the direct read-out of the PTB-SQUIDs a very low-noise pre-amplifier (LNA), T_N < 30K, is required, while for the read-out of the other SQUIDs the use of 2nd-stage array-SQUIDs relaxes the demand on the LNA. Furthermore the FEE-box contains all DC-supply sources for the various SQUIDs and the cold FLL-electronics. In one out of the two electronic channels we will test cold FLL-electronics, allowing for a very low-noise LNA and a significant reduction of cable length thereby enhancing the FLL-gain-bandwidth. Initial developments of that cold electronics looks quite promising[23,24], but it remains to be seen if the power dissipation at cryogenic temperatures is commensurate with space applications.

Baseline however is to develop digital baseband feedback, since that promises more favorite performance over a much wider frequency range

Digital electronics and AC-bias generation is explicitly placed elsewhere to minimize risk of energy resolution degradation due to high frequency disturbances.

4.4.2 AC-Bias Cards

The AC-bias generators inside the electronics rack have stringent signal-to-noise requirements, i.e. a – 120dBc/Hz amplitude to noise ratio at 100 Hz - 2 kHz from the carrier frequency. The phase-noise requirements are significantly (about 30dB) less demanding. Digital generation of these carriers in so-called Direct Digital Synthesis (DDS) chips does meet those specifications at the cost of high power consumption. The AC-bias boards have been made and tested and they do meet the very demanding carrier to noise ratio.

In parallel we have studied and tested the generation of AC-bias carriers directly inside the FPGA on the de-multiplexing board. The Cordic algorithm seems quite suitable and able to reach the required specifications when making use of xxx bits and xxx MSa/s. Obviously a high quality DAC is required to transfer the output to an analogue bias signal.

4.4.3 De-Multiplication and Command & Control cards

The DEMUX-card contains two 16-bit 100 MSa/s ADC's to convert the analogue data into digital. The actual requirement on the ADC number of bits is significantly smaller when used in the forward part of the base-band feedback loop. So the ADC's used are significantly overrated in this phase of the program. Subsequently an FPGA on the DEMUX-board will be used for digital de-multiplication, filtering, and remodulation to create the base band feedback loop. The total digital delay due to ADC, FPGA calculations, and DAC is about 150 ns. The delay due to phase rotation in amplifiers and filters is approximately equal, making the total delay about 300 ns.

The demuxcard is presently programmed and tested and expected to be available for the first FDM measurements with 1 – several pixels by autumn this year.

4.5 Electrical Ground Support Equipment and Data Analysis

The instrument is controlled by a PC-based EGSE coupled to the EURECA instrument by means of optical links. The system is designed such that at least one of the DEMUX cards can dump its raw data (350 kBits/s) directly on the disk of the PC, while the other channel will transport a significantly reduced data rate from the other demux cards. The EGSE enables automatic test procedures and command logging. Obviously the EGSE also allows for quick look analysis of some of the data during accumulation in order to have direct access to the quality of the data.

The partners at IDSC, Geneva and IFC, Santander are developing an offline data analysis facility making use of the heritage of the Integral Data Analysis and expanding it with the analysis tools and algorithms required to analyse and TES-characterization data, TES-science data. The data input is in FITS format.

5. SUMMARY

EURECA is a powerful means to demonstrate technical readiness for the deployment of TES-based imaging spectrometers in space. A first successful campaign at PTB facility of the BESSY synchrotron has shown single pixel performance of 1.5 eV at 250 eV, and 2.5 eV @ 5.9 keV. The project aims to prove the FDM performance with base-band feedback within the coming year. The deployment of cold electronics with a very short FLL will be tested as a back-up. Extensive X-ray calibration of the instrument at the BESSY synchrotron beam line using FDM with base-band feedback for the read-out of the 5 x 5 pixel array is foreseen begin 2010.

6. ACKNOWLEDGEMENTS

The authors acknowledge an ESA Technological Research Program contract for the development of TES-arrays and SQUIDs, being a significant support to the EURECA program. Also the recent ESA TRP contract for the development of SQUID-based electronics is of crucial importance for this work.

7. REFERENCES

1. M.P. Bruijn, N.H.R. Baars, W.M. Bergmann Tiest, A. Germeau, H.F.C. Hoevers, P.A.J. de Korte, W. A. Mels, M.L. Ridder, E. Krouwer, J.J. van Baar, R.J. Wiegerink, “Development of an array of transition edge sensors for application in X-ray astronomy”, in Proceedings of the 10th International Workshop on Low Temperature Detectors - LTD-10, F. Gatti Eds., *Nucl. Instr. and Meth. A*, 520, 443-445 (2004)
2. P.A.J. de Korte, J.J. van Baar, N.H.R. Baars, F.E. Bakker, W. M. Bergmann Tiest, M.P. Bruijn, A. Germeau, H.F.C. Hoevers, M. Kiviranta, E. Krouwer, J. van der Kuur, M.P. Lubbers, W.A. Mels, M.L. Ridder, H. Seppä, and R.J. Wiegerink,”A cryogenic imaging X-ray spectrometer for XEUS read out by frequency-division SQUID multiplexers”, *Proceedings SPIE*, 5501, 167 – 176 (2004)
3. J.N. Ullom, J.A. Beall, W.B. Doriese, W.D. Duncan, L.Ferreira, G.C. Hilton, K.D. Irwin, C.D. Reintsema, L.R. Vale, “Optimized transition-edge x-ray micro-calorimeter with 2.4 eV energy resolution at 5.9 keV”, *Appl. Phys. Lett.*, 87, 194103 (2005)
4. A. T. Lee, “SQUID readout multiplexers for transition-edge sensor arrays“, in Proceedings of the 11th International Workshop on Low Temperature Detectors - LTD-11, M. Ohkubo, K. Mitsuda and H. Takahashi Eds., *Nucl. Instr. and Meth. A,* 559, 786-789 (2006)
5. C. D. Reintsema, J. Beyer, Sae Woo Nam, S. Deiker, G. C. Hilton, K. Irwin, J. Martinis, J. Ullom, and L. R. Vale,“Prototype system for superconducting quantum interference device multiplexing of large-format transition-edge sensor arrays”, *Rev. Sci. Instrum.*, 74, 4500-4508 (2003)
6. P. A. J. de Korte, J. Beyer, S. Deiker, G. C. Hilton, K. D. Irwin, M. MacIntosh, Sae Woo Nam, C..D. Reintsema, and L. R. Vale, “Time-division superconducting quantum interference device multiplexer for transition-edge sensors”, *Rev. Sci. Instrum.,* 74, 3807-3815 (2003)

7. W.B. Doriese, J.A. Beall, W.D. Duncan, L. Ferreira, G.C. Hilton, K.D. Irwin, C.D. Reintsema, J.N. Ullom, L.R. Vale, Y. Xu,"Progress toward kilopixel arrays: 3.8 eV microcalorimeter resolution in 8-channel SQUID multiplexer", in Proceedings of the 11th International Workshop on Low Temperature Detectors - LTD-11, M. Ohkubo, K. Mitsuda and H. Takahashi Eds., *Nucl. Instr. and Meth. A*, 559, 808-810 (2006)
8. T. M. Lanting, Hsiao-Mei Cho, John Clarke, W. L. Holzapfel, Adrian T. Lee, M. Lueker, P. L. Richards, Matt A. Dobbs, Helmuth Spieler, and A. Smith, "Frequency-domain multiplexed readout of transition-edge sensor arrays with a superconducting quantum interference device", *Appl. Phys. Lett.,* 86, 112511 (2005)
9. N. Iyomoto, T. Ichitsubo, K. Mitsuda, N.Y. Yamasaki, R. Fujimoto, T. Oshima, K. Futamoto, Y. Takei, T. Fujimori, K. Yoshida, Y. Ishisaki, U. Morita, T. Koga, K. Shinozaki, K. Sato, N. Takai, T. Ohashi, T. Miyazaki, S. Nakayama, K. Tanaka, T. Morooka, K. Chinone, "Frequency-domain multiplexing of TES microcalorimeter array with CABBAGE", in Proceedings of the 10th International Workshop on Low Temperature Detectors - LTD-10, F. Gatti Eds., *Nucl. Instr. and Meth. A*, 520, 566-569 (2004)
10. M. Kiviranta, H. Seppae, J. van der Kuur, J., and P. de Korte,"SQUID-based read-out schemes for microcalorimeter arrays," in *AIP Conf. Proc. LTD-9*, F. Porter, D. McCammon, M. Galeazzi, and C. Stahle Eds., 605, 295-300 (2001)
11. J. van der Kuur, P.A.J. de Korte, P. de Groene, N.H.R. Baars, M.P. Lubbers, M. Kiviranta," Implementation of frequency domain multiplexing in imaging arrays of microcalorimeters", in Proceedings of the 10th International Workshop on Low Temperature Detectors - LTD-10, F. Gatti Eds., *Nucl. Instr. and Meth. A*, 520, 551-554 (2004)
12. J. van der Kuur, P. A. J. de Korte, H. F. C. Hoevers, M. Kiviranta, and H. Seppae," Performance of an x-ray microcalorimeter under ac biasing", *Appl. Phys. Lett.*, 81, 4467 – 4469 (2002)
13. M. F. Cunningham, J. N. Ullom, T. Miyazaki, S. E. Labov, John Clarke, T. M. Lanting, Adrian T. Lee, P. L. Richards, and Jongsoo Yoon," High-resolution operation of frequency-multiplexed transition-edge photon sensors", *Appl. Phys. Lett*., 81, 159-161 (2002)
14. Jongsoo Yoon, J. Clarke, J. M. Gildemeister, A.T. Lee, M. J. Myers, P. L. Richards, and J. T. Skidmore," Single superconducting quantum interference device multiplexer for arrays of low-temperature sensors", *Appl. Phys. Lett*., 78, 371-373 (2001)
15. K. Mitsuda, R. Fujimoto, T. Miyazaki, K. Maegami, Y. Aruga, T. Oshima, S. Nakayama, S. Shoji, H. Kudo, Y. Yokoyama, T. Mihara, H.M. Shimizu,"Multi-pixel readout of transition-edge sensors using a multi-input SQUID", *Nucl. Instr. and Meth. A.,* 436, pp. 252-255, 1999
16. N.Y. Yamasaki, K. Masui, K. Mitsuda, T. Morooka, S. Nakayama, Y. Takei, "Design of frequency domain multiplexing of TES signals by multi-input SQUIDs", in Proceedings of the 11th International Workshop on Low Temperature Detectors - LTD-11, M. Ohkubo, K. Mitsuda and H. Takahashi Eds., *Nucl. Instr. and Meth. A*, 559, 790-792 (2006)
17. M. Kiviranta, J. S. Penttilä, L. Grönberg, J. Hassel, A. Virtanen, and H. Seppä, "Design and performance of multiloop and washer SQUIDs intended for sub-kelvin operation", *Supercond. Sci. Technol.,* 17, S285-S289 (2004)
18. D. Drung, C. Hinnrichs, and H.-Jobes Barthelmess,"A low-noise ultra-high-speed dc SQUID readout electronics", *Supercond. Sci. Technol*., 19, S235-S241 (2006)
19. D. Drung, C. Aßmann, J. Beyer, A. Kirste, M. Peters, F. Ruede, and Th. Schurig, "Highly sensitive and easy-to-use SQUID sensors", *IEEE Transactions on Applied Superconductivity.,* 17, 699 – 704 (2007)
20. D. Drung," High-Tc and low-Tc dc SQUID electronics", Supercond. Sci. Technol., vol.16, pp. 1320-1336, 2003
21. K. Irwin, K., G. Hilton, G.,"Transition-Edge Sensors", in *Cryogenic Particle Detection*, Christian Enns Eds., Series: Topics in Applied Physics, Springer Verlag, ISBN: 3-540-20113-0, 99, 63 – 149 (2005)
22. Sae Woo Nam and Joel Ullom, private communication, 2005
23. M. Kiviranta, A. Virtanen, H. Seppä, J. Penttilä, J. Hassel, and P. Helistö, "A post-SQUID ac amplifier aimed for multiplexed detector read-outs", *Supercond. Sci. Technol.*, 19, S371-S375 (2006)
24. D. Drung, C. Hinnrichs, and H.-J. Barthelmess, to be presented at ASC 2006